HHS Public Access

Author manuscript

Exp Eye Res. Author manuscript; available in PMC 2018 November 01.

Published in final edited form as:

Exp Eye Res. 2017 November ; 164: 118–128. doi:10.1016/j.exer.2017.08.007.

Inhibition of HUVEC tube formation via suppression of NFκB suggests an anti-angiogenic role for SLURP1 in the transparent cornea

Sudha Swamynathan[a], **Chelsea L. Loughner**[a], and **Shivalingappa K. Swamynathan**[a,b,c,d,*]

[a]Department of Ophthalmology, University of Pittsburgh School of Medicine, Pittsburgh, USA

[b]Department of Cell Biology, University of Pittsburgh School of Medicine, Pittsburgh, USA

[c]McGowan Institute of Regenerative Medicine, University of Pittsburgh, USA

[d]Fox Center for Vision Restoration, University of Pittsburgh School of Medicine, Pittsburgh, USA

Abstract

Previously, we have reported that the Secreted Ly6/uPAR related protein-1 (SLURP1) serves an important immunomodulatory function in the ocular surface. Here, we examine the involvement of SLURP1 in regulating corneal angiogenic privilege. Slurp1 expression detected by QPCR, immunoblots and immunofluorescent stain, was significantly decreased in mouse corneas subjected to alkali burn-induced corneal neovascularization (CNV). Addition of exogenous SLURP1 (6XHis-tagged, E. coli expressed and partially purified using Ni-ion columns) significantly suppressed the tumor necrosis factor-α (TNF-α)- stimulated human umbilical cord vascular endothelial cell (HUVEC) tube formation. SLURP1 suppressed the HUVEC tube length, tube area and number of branch points, without affecting their viability and/or proliferation. Exogenous SLURP1 in HUVEC also suppressed the TNF-α-induced (*i*) interleukin-8 (IL-8) and TNF-α production, (*ii*) adhesion to different components of the extracellular matrix, *(iii)* migration, and (*iv*) nuclear localization of NFκB. Together, these results demonstrate that SLURP1 suppresses HUVEC tube formation by blocking nuclear translocation of NFκB, and suggest a potential role for SLURP1 in promoting corneal angiogenic privilege.

Keywords

SLURP1; Corneal epithelium; Inflammation; Angiogenic privilege; NFκB; HUVEC

*Corresponding author. University of Pittsburgh School of Medicine, Eye and Ear Institute, 203 Lothrop Street, Room 1025, Pittsburgh PA 15213, USA. Swamynathansk@upmc.edu (S.K. Swamynathan).

Author contributions

S.S. conceived and performed the experiments with HUVEC. C.L.L. and S.K.S. performed the alkali burn experiments in mouse corneas. S.S. and S.K.S. conceived the experiments, analyzed the results and wrote the manuscript. All authors have read and approved the final version of the manuscript.

Conflict of interest disclosures

S. Swamynathan (Patent); S.K. Swamynathan, (Patent); C.L. Loughner, None.

1. Introduction

Corneal avascularity-a primary requirement for the cornea to remain transparent-is regulated by several distinct and redundant mechanisms that work in concert (Azar, 2006; Barabino et al., 2012; Bock et al., 2013; Clements and Dana, 2011). Corneal angiogenic privilege depends on the counterbalance between pro-angiogenic factors such as vascular endothelial growth factor-A (VEGF-A), VEGF-C, tumor necrosis factor alpha (TNF-α) and anti-angiogenic factors such as soluble VEGF Receptor-1 (VEGF-R1), VEGF-R3, programmed death ligand-1 (PD-L1), pigment epithelium derived factor (PEDF), angiostatin, endostatin, thrombospondin-1 (TSP1) and TSP2 (Ambati et al., 2006; Azar, 2006; Clements and Dana, 2011; Cursiefen et al., 2005; Fibbi et al., 1998; Jin et al., 2011; Ma et al., 2006; Stuart et al., 2003). In pro-inflammatory conditions, this balance shifts towards pro-angiogenic factors, resulting in the in growth of blood and lymph vessels into the cornea followed by edema and loss of visual acuity. Angiogenic inflammation of the cornea is a major cause of corneal blindness in the world (Clements and Dana, 2011; Lee et al., 1998). Despite recent progress, our understanding of the molecular mechanisms governing corneal angiogenic privilege remains incomplete.

The secreted Ly6/uPAR-related protein-1 (SLURP1) is an 88 amino acids member of the leukocyte antigen-6 (Ly6) family of proteins (Loughner et al., 2016). SLURP1 is expressed abundantly in the cornea and moderately in oral mucosa, skin and other epithelia, where it is secreted into tear, saliva, sweat, and urine (Adermann et al., 1999; Norman et al., 2004). It is also expressed in bronchial epithelial cells, a variety of immune cells, primary sensory neurons, and the retina (Fujii et al., 2014; Horiguchi et al., 2009; Mastrangeli et al., 2003; Matsumoto et al., 2012; Moriwaki et al., 2007, 2009). SLURP1 is a ligand of α7-nAchR and a late marker of epidermal differentiation (Chimienti et al., 2003; Favre et al., 2007; Horiguchi et al., 2009). Mutations or deletions in *SLURP1* cause hyperkeratotic palmoplantar disorder Mal-de-Meleda (Eckl et al., 2003; Fischer et al., 2001; Hu et al., 2003; Ward et al., 2003). *Slurp1*-null mice develop severe palmoplantar keratoderma with elevated keratinocyte proliferation, reduced adiposity, protection from obesity on a high-fat diet, and accumulation of lipid droplets in the stratum corneum, reminiscent of Mal-de-Meleda (Adeyo et al., 2014). Previously, we reported that Slurp1 serves as an immunomodulatory switch that keeps the cornea free of inflammation and is rapidly downregulated in pro-inflammatory conditions allowing helpful inflammation when needed (Swamynathan et al., 2012, 2015; Swamynathan and Swamynathan, 2014). We also demonstrated that SLURP1 modulates corneal homeostasis by serving as a soluble scavenger of urokinase-type plasminogen activator (uPA) (Swamynathan and Swamynathan, 2014). The immunomodulatory role of SLURP1 and the redundant nature of diverse pathways that govern corneal avascularity raise the possibility that SLURP1 plays a role in maintaining the cornea avascular. Consistent with this possibility, genome-wide comparison of gene expression in sutureand alkali burn-induced murine corneal neovascularization (CNV) identified *Slurp1* as one of the highly downregulated genes, strongly implying its involvement in regulation of corneal angiogenic privilege (Jia et al., 2011). Here, we have examined the role of SLURP1 in regulating angiogenesis by evaluating its effect on human umbilical cord vascular endothelial cell (HUVEC) tube formation *in vitro*. The results

presented here demonstrate that SLURP1 suppresses HUVEC tube formation by blocking nuclear translocation of NFκB, and suggest a potential role for SLURP1 in corneal angiogenic privilege.

2. Materials and methods

2.1. Cells and reagents

Primary HUVEC cells from pooled donors were obtained from Lonza (Portsmouth, NH) and maintained in Endothelial Growth Medium-2 (EGM2). Recombinant human SLURP1 was expressed in E. coli and partially purified on Ni-ion columns. Mock purified protein from an E. coli strain without SLURP1 expression vector served as control protein (CP). TNF-α was purchased from Thermo Scientific (Pittsburgh, PA), Vitronectin from Peprotech (Rocky Hill, NJ), Collagen-1 from BD Biosciences (San Jose, CA), Collagen-IV and Matrigel-GFR from Corning (Corning, NY), and Fibronectin from Sigma-Aldrich (St Louis, MO).

2.2. Corneal angiogenesis by alkali burn

Alkali burn-induced CNV, widely used for studying angiogenic inflammation (Jia et al., 2011; Kubota et al., 2011; Parikh et al., 2011; Yoshizuka et al., 1981), was used to induce corneal angiogenesis in 8- to 10-week old mice of mixed background. Mice were anesthetized by intraperitoneal injection of a mix of ketamine and xylazine. Proparacaine eye drops were used to further anesthetize the corneas. Filter discs soaked in 1.0 M NaOH were placed on central cornea for 20 s, rinsed thoroughly with a gentle stream of 20 ml phosphate buffered saline (PBS) and allowed to recover. Progression of alkali burn-induced angiogenesis was tracked by imaging the corneas on days 0, 2, 7 and 13 post-alkali exposure using a slit-lamp biomicroscope. Corneal expression of Slurp1 at these time points was measured by QPCR, immunoblots and immunofluorescent stain as before (Swamynathan et al., 2015). Mice used in these experiments were housed in an AAALAC-approved animal facility. All procedures were approved by the University of Pittsburgh Institutional Animal Care and Use Committee (IACUC protocol# 15066259) and conformed to the guidelines set by the Association for Research in Vision and Ophthalmology (ARVO).

2.3. HUVEC tube formation assay

We used HUVEC tube formation assay, which measures the ability of endothelial cells plated at sub-confluent densities with the appropriate extracellular matrix support, to form capillary-like structures (tubes) to model the reorganization stage of angiogenesis. HUVEC cells were maintained in endodermal growth medium-2 (EGM2). Cells in passages P3 to P6 were pre-treated with TNF-α (10 ng/ml), and SLURP1 (1 μg/ml) or vehicle control for 15 min in endodermal basal medium-2 (EBM2) + 0.25% Fetal Calf Serum. Pretreated cells were seeded on Matrigel-GFR (Growth Factor reduced) with or without SLURP1. Tubes were allowed to form for 18–24 h at 37 °C in a humidified chamber with 5% CO_2 in air. Fluorescent images were captured after staining with Calcein-AM, and analyzed using MetaMorph software (Molecular Devices; Sunnyvale, CA).

2.4. HUVEC viability assay

HUVEC cells were plated at a density of 25×10^3 cells per well in a 96-well plate in EGM2. After the cells adhered, TNF-α and SLURP1 was added in EBM2+0.5% FBS. After 24 h, the number of viable cells was measured by adding Celltiter blue, incubating for 1 h in CO_2 incubator and measuring fluorescence at 590 nm with excitation set at 530 nm.

2.5. HUVEC proliferation assay

HUVEC cells were seeded in a 96 well plate at a density of 5×10^3 cells per well in EGM2 and allowed to adhere overnight. Medium was changed to EBM2 with 0.5% FBS for 6 h and then treated with 10 ng/ml TNF-α and 1 μg/ml SLURP1. The number of cells was measured after 24 h using Celltiter blue as above.

2.6. RNA extraction, reverse transcription and QPCR

Relative expression of cytokines was quantified by QPCR 4 h after SLURP1 or control protein pretreated HUVEC cells were exposed to 10 ng/ml TNF-α. Total RNA was isolated using EZ-10 spin column total RNA mini-prep kit from Bio Basic Inc. (Amherst, NY), 300 ng of which was used for cDNA synthesis with Mouse Moloney Leukemia Virus reverse transcriptase (Promega, Madison, WI). SYBR Green gene expression assays were performed in triplicate in ABI StepOne Plus thermocycler with validated primers from realtimeprimers.com (Elkins Park, PA) using 18S rRNA, RPL13A or Actin-B as endogenous control. QPCR results were analyzed using StepOne software (Applied Biosystems). Results shown are the average of three independent experiments.

2.7. Adhesion assay

HUVEC cells maintained overnight in EBM2+0.5% serum were dissociated using accutase, pre-incubated with control protein or SLURP1 for 30 min followed by incubation with or without TNF-α for 30 min. Treated HUVEC cells seeded in a 96-well plate coated with Collagen-1 (5 μg/cm^2), Collagen-IV (2), Fibronectin (2 μg/cm^2), Vitronectin (0.2 μg/cm^2) or BSA (2 μg/cm^2), were allowed to adhere for 30 min in humidified CO_2 incubator. Adherent HUVEC cells were stained by crystal violet and relative adherence measured by solubilizing crystal violet in 20% acetic acid and measuring absorbance at 590 nm using Biotek Synergy-II plate reader (Biotek Instruments, Winooski, VT).

2.8. Gap filling assays

A gap was introduced in confluent HUVEC cells with a 200 μl tip. The cells were then washed with PBS and incubated in EBM2+0.5% FBS with 1 μg/ml control protein or SLURP1 in the presence or absence of 10 ng/ml TNF-α. Four distinct areas of the gaps were photographed immediately after gap generation (0 h) and 18 h later, using a Nikon TS100 inverted microscope with a 2X objective and a Spot RT camera (Diagnostics Instruments; Sterling Heights, MI) and quantified by MetaMorph. The images were taken at the same spot at 0 and 18 h after wounding using reference markings just outside of the imaged area.

2.9. Immunoblots

Mice were euthanized by CO_2 asphyxiation followed by cervical dislocation at indicated time points after alkali-burn, and corneal lysate was prepared by homogenizing dissected corneas in RIPA buffer (10 mM Tris-Cl (pH 8.0), 1 mM EDTA, 1% Triton X-100, 0.1% Sodium deoxycholate, 0.1% SDS, 140 mM NaCl and 1 mM PMSF). Equal amount of protein quantified by bicinchoninic acid (BCA) (Pierce, Rockford, IL) method was separated on NuPage 4–12% acrylamide gradient gels using MES SDS running buffer (Invitrogen, Carlsbad, CA), transferred to polyvinylidene difluoride (PVDF) membranes and probed with 1:200 dilution of rabbit anti-mouse Slurp1 antibody (a kind gift from Dr. Misawa, Keio University, Tokyo, Japan) (Moriwaki et al., 2009; Swamynathan et al., 2012). IRDye-800 goat anti-rabbit secondary antibody was used to detect primary antibody-bound protein bands using Odyssey scanning system from LI-COR (Lincoln, NE). The membrane was re-probed with goat anti-actin antibody (Santa Cruz Biotechnology, Santa Cruz, CA. catalog # sc 1616, Lot #D0609) and IRDye-680 donkey anti-goat antibody to ensure equal loading.

For NFκB nuclear translocation studies, HUVEC cells were grown overnight in EBM2+0.5% FBS and pre-treated with control protein or SLURP1 for 30 min and then exposed to TNF-α (10 ng/ml) for 10, 20 or 30 min. Nuclear protein was extracted using nuclear extraction buffer (20 mM HEPES, 500 mM NaCl, 0.2 mM EDTA, 0.5 mMDTT, 1.5 mM MgCl2, 1 mM PMSF) and quantified by BCA method. Equal quantities of nuclear protein were electrophoresed and transferred to PVDF membranes as above, and probed with 1:1000 dilution of mouse anti-NFκB antibody (Cell Signaling Technology, Danvers MA. Catalog # 6956, Lot # 6). IRDye goat anti-mouse secondary antibody was used to detect primary antibody-bound protein bands as above. Membranes were stripped of the antibody with 1x stripping buffer (NewBlot IR Stripping buffer, LICOR part # 929-40028) for 15 min at room temperature on a rocker, washed 3 times with PBS (5 min each) and re-probed with anti-TATA binding protein antibody (Cell Signaling Technology, Catalog # 44069; Lot # 1) to ensure equal loading of nuclear extract.

2.10. Immunofluorescent stain

HUVEC cells grown on vitronectin-coated glass cover slips in EBM2+0.5% FBS were pre-treated with control protein or SLURP1 for 30 min and exposed to TNF-α (10 ng/ml) for additional 10, 20 or 30 min, fixed in buffered 3% paraformaldehyde for 20 min, washed thrice for 5 min each with PBS, permeabilized with 0.1% triton in PBS, washed thrice with PBS for 5 min each, blocked with 10% goat serum in PBS for 1 h at room temperature in a humidified chamber, washed twice with PBS for 5 min each, incubated with a 1:500 dilution of the mouse anti-NFκB primary antibody overnight in a humidified chamber at 4 °C, washed thrice with PBS for 5 min each, incubated with secondary antibody (Alexafluor 488-coupled goat anti-mouse IgG from Molecular Probes, Carlsbad, CA) at a 1:300 dilution for 1 h at room temperature, washed thrice with PBS containing 0.1% Tween-20 (PBST) for 5 min each, counter-stained with 4′,6-diamidino-2-phenylindole (DAPI), and coverslipped using Aqua-Poly/Mount (Polysciences, Warrington, PA). After drying overnight, the coverslips were sealed with clear nail polish and the images collected using Olympus IX81 confocal microscope.

3. Results

3.1. Slurp1 is downregulated during alkali burn-induced corneal neovascularization

We utilized alkali burn-a well-established model of corneal angiogenesis (Jia et al., 2011; Kubota et al., 2011; Yoshizuka et al., 1981; Zhang et al., 2006)- to determine how Slurp1 expression changes during angiogenic inflammation. CNV was evident by 7 days post-alkali burn and was retained at 13 days post-alkali burn (Fig. 1A). QPCR revealed and immunoblots confirmed that Slurp1 expression was significantly downregulated at 2, 7 and 13 days post-alkali burn, compared with that in the naïve contralateral eyes (Fig. 1B and C). Consistent with these results, immunofluorescent stain revealed abundant expression of Slurp1 in the contralateral corneal epithelium, but not the alkali-burned corneas (Fig. 1D). Alkali-burned corneal stroma was edematous and contained on average, 23,950, 18,153 and 23,605 cells per mm^2 of stroma at days 2, 7 and 13 respectively, compared with 2,885, 2894 and 4030 per mm^2 stroma in control corneas, indicating significant immune infiltrate in alkali-burned corneas ($n = 4$; $p = 0.014$, 0.0001, and 0.0037, respectively). Together, these results reveal that Slurp1 is significantly downregulated during alkali-burn induced CNV, indicating a potential role for Slurp1 in regulating corneal angiogenic inflammation.

3.2. SLURP1 suppresses HUVEC tube formation

Next, we employed *in vitro* HUVEC tube formation assays to directly determine the effect of SLURP1 on angiogenesis. Control protein-treated HUVEC cells formed tubes in the absence of any additional stimulation when plated in EBM2+0.25% FBS in matrigel-GFR (Fig. 2A). Addition of recombinant SLURP1 partially suppressed HUVEC tube formation (Fig. 2B). Addition of TNF-α further stimulated HUVEC tube formation, which was efficiently inhibited by SLURP1 (Fig. 2C and D). Morphometric measurements from six independent replicates revealed that the inclusion of TNF-α increased the mean HUVEC tube length, tube area and number of branch points (Fig. 2E–G). Addition of SLURP1 partially suppressed the HUVEC tube length, tube area, and the number of branch points. The extent of this suppression was more, and statistically significant when SLURP1 was added to the TNF-α-stimulated HUVEC cells (Fig. 2E–G). The viability and proliferation of HUVEC cells were not significantly affected by SLURP1 (Fig. 3A and B), suggesting that SLURP1-mediated suppression of HUVEC tube formation is not an indirect outcome of their decreased viability and/or proliferation. Taken together, these results suggest that SLURP1 suppresses TNF-α-stimulated HUVEC tube formation without altering their viability or proliferation.

3.3. SLURP1 suppresses the TNF-α-induced expression of IL-8 and TNF-α in HUVEC

To determine if cytokine expression is affected following alkali burn in the cornea, we examined the relative levels of cytokine transcripts in 2- and 7-day-post-alkali-burned mouse corneas. We observed elevated expression of transcripts encoding proinflammatory cytokines Ifna, Ifnb, Cxcl1, Cxcr2 and Tnfa in mouse corneas at days 2 and 7 post-alkali-burn (Fig. 4A), consistent with the previous studies that reported similar upregulation (Saika et al., 2005; Sotozono et al., 1997). Considering that TNF-α is a potent cytokine that exerts its effects by stimulating the expression of a host of other cytokines, we measured the effect of SLURP1 on expression of different cytokines in HUVEC pre-treated with control protein

or SLURP1, followed by TNF-α for 4 h. QPCR revealed that the expression of IL-8 was highly stimulated by TNF-α, and that this stimulationwas subdued in the presence of SLURP1 in HUVEC (Fig. 4B). Similarly, auto-stimulation of TNF-α expression in TNF-α-treated HUVEC cells was subdued by SLURP1 treatment (Fig. 4B). The expression of other cytokines tested was not affected by TNF-α and SLURP1. Thus, SLURP1-mediated suppression of HUVEC tube formation is associated with decreased expression of IL-8 and TNF-α.

3.4. SLURP1 modulates HUVEC interaction with the extracellular matrix, and migration

As angiogenic potential of the endothelial cells depends on both their interaction with the extracellular matrix (ECM) and their ability to migrate through the ECM, we evaluated the effect of SLURP1 on interaction of HUVEC cells with ECM components. Relative to control protein, treatment with either SLURP1 or TNF-α alone suppressed the adhesion of HUVEC cells to collagen-1-, collagen-4-vitronectin-, or fibronectin-coated plates. Treatment with both SLURP1 and TNF-α further decreased the affinity of this interaction with collagen-4, vitronectin and fibronectin (Fig. 5). Next, we determined the effect of SLURP1 on HUVEC cell migration in gap filling assays. TNF-α stimulated HUVEC cell migration, while addition of SLURP1 suppressed it (Fig. 6). Together, these results suggest that SLURP1 modulates HUVEC cell interaction with the ECM, and their migration.

3.5. SLURP1 suppresses TNF-α-stimulated nuclear translocation of NFκB

Considering that the stress-activated transcription factor NFκB is a major participant in TNF-α-stimulated angiogenic inflammation (Reynolds et al., 2014), we examined if TNF-α-triggered nuclear localization of NFκB is affected in HUVEC cells. Immunoblots revealed efficient nuclear translocation of NFκB upon TNF-α treatment, which was suppressed in HUVEC cells exposed to SLURP1 (Fig. 7A and B). Uniformity in nuclear extract preparation and loading was ensured by re-probing with anti-TBP antibody as control (Fig. 7A and B). Next, we pre-treated the HUVEC cells with control protein or SLURP1 for 30 min, exposed to TNF-α, and fixed at 0, 10, and 30 min after TNF-α treatment, and the sub-cellular localization of NFκB was evaluated by immunofluorescent staining. Treatment with TNF-α induced nuclear localization of NFκB in control protein treated HUVEC cells within 10 min but not in SLURP1-treated cells, where it remained largely within the cytoplasm even after 30 min of treatment (Fig. 7C). Together, these results suggest that SLURP1 suppresses TNF-α-stimulated nuclear translocation of NFκB in HUVECs.

4. Discussion

Corneal angiogenic privilege depends on the balance between proangiogenic and antiangiogenic factors (Azar, 2006; Clements and Dana, 2011). The normally avascular cornea may vascularize when the equilibrium between pro- and anti-angiogenic factors is tilted towards pro-angiogenic factors resulting in the growth of new blood vessels from pre-existing vasculature at the pericorneal plexus. In view of the critical role of the cornea in ensuring proper vision, it is important to identify the different molecular mechanisms that regulate corneal angiogenic privilege. In this report, we have presented evidence that Slurp1, one of the most abundantly expressed proteins in the cornea, is sharply downregulated in the

alkali burn model of mouse CNV, and that in HUVEC cells cultured *in vitro*, SLURP1 suppresses TNF-α-stimulated *(i)* tube formation (tube length, area and number of branch points) without affecting their survival and/or proliferation, *(ii)* IL-8, and TNF-α production, *(iii)* rate of cell migration, *(iv)* adhesion to different ECM components, and *(v)* nuclear localization of NFκB. Consistent with our observations, comparison of genome-wide gene expression in both suture- and alkali burn-induced CNV detected *Slurp1* mRNA as one of the highly downregulated genes (Jia et al., 2011). Together, these results indicate a potential role for SLURP1 in corneal angiogenic privilege by blocking nuclear translocation of NFκB, a key transcription factor that regulates cellular responses to proinflammatory stimuli (Fig. 8).

Fitting with the essential nature of corneal transparence for vision, pro- and anti-angiogenic factors have been studied intensively, revealing the important role of innate immune cells in CNV. For instance, CD11b+macrophages are required for corneal lymphangiogenesis under pathological conditions (Maruyama et al., 2005, 2012). Similarly, Th17 cells promote angiogenesis in autoimmune diseases and malignancies through IL-17 (Chauhan et al., 2011). In contrast, cell surface molecules FAS-L, VEGF-R3 and PD-L1, as well as secreted molecules TGFβ and soluble VEGF-R1 promote corneal avascularity by inhibiting infiltration and angiogenic activity of leukocytes (Ambati et al., 2006; Azar, 2006; Cursiefen et al., 2006; El Annan et al., 2010; Jin et al., 2011; Keir et al., 2008; Morris et al., 2012; Stuart et al., 2003; Tandon et al., 2010). Though the present data coupled with our previous reports (Swamynathan et al., 2012, 2015; Swamynathan and Swamynathan, 2014) suggest that SLURP1 is an important secreted component of the corneal innate immune response, in vivo experiments with *Slurp1*-knockout mouse corneas would be necessary to provide definitive evidence in favor of the role of Slurp1 as an anti-angiogenic molecule. HUVEC-derived data presented here only provide proof of concept that SLURP1 is a potentially valuable target for managing diseases involving corneal neovascularization. The in vivo relevance and applicability of these findings remain to be established.

Inflammation is the common denominator in CNV induced by microbial infection, chemical injury, autoimmune disorders, contact lens induced irritation, and post-corneal transplant complications (Clements and Dana, 2011; Lee et al., 1998). Previously, we suggested an immunomodulatory role for Slurp1 in the mouse cornea based on our findings that (*i*) corneal expression of Slurp1 is abrogated upon Herpes Simplex Virus type-1 (HSV-1) infection, corneal exposure to bacterial lipopolysaccharide (LPS) or fungal cell wall zymosan-A, concurrent with neutrophil infiltration, and (*ii*) SLURP1 is downregulated in human corneal limbal epithelial cells exposed to pro-inflammatory interleukins IL-4 and IL-13 (Swamynathan et al., 2012, 2015). In adenoviral keratitis model of mouse corneal inflammation, over-expression of Slurp1 hindered neutrophil influx into corneas, providing further support for the immunomodulatory function of Slurp1 (Swamynathan et al., 2012). We also demonstrated that Slurp1 serves as a soluble scavenger of urokinase, the ligand for urokinase-type plasminogen activator receptor (uPAR) that plays a critical role in angiogenic inflammation (Blasi and Carmeliet, 2002; Montuori and Ragno, 2014; Smith and Marshall, 2010; Swamynathan and Swamynathan, 2014). The present data, that SLURP1 suppresses HUVEC tube formation by blocking NFκB activity, further bolsters the role of SLURP1 as an immunomodulatory molecule.

Aberrant cell proliferation, migration, and interaction with ECM are key features of angiogenic inflammation associated with corneal pathologies (Azar, 2006; Clements and Dana, 2011; Lim et al., 2009). Treatment of HUVEC cells with either SLURP1 or TNF-α suppressed their adhesion to collagen-1-, collagen-4-, vitronectin-, or fibronectin-coated plates (Fig. 5). This inhibitory effect was enhanced when they both were treated together. These results are consistent with the previous reports that TNF-α inhibits human endothelial cell adhesion to vitronectin, laminin, and fibronectin by suppressing the expression of $\alpha_v\beta_3$ integrin (Defilippi et al., 1991), $\alpha_6\beta_1$ integrin (Defilippi et al., 1992), and $\alpha_5\beta_1$ integrin (Rotundo et al., 2002). Whether SLURP1 has a similar inhibitory effect on expression of these or other integrins remains to be determined.

An important observation in this study is that SLURP1 blocks HUVEC tube formation by suppressing nuclear localization of NFκB (Fig. 7). Several studies in the past have addressed the changes in cytokine expression and nuclear translocation of NFκB following alkali burn in the mouse corneas. Cytokines IL-1α, IL-1β, IL-6, IL-10 and TNF-α are overexpressed in alkali-burned corneas (Sotozono et al., 1997). Consistent with the involvement of NFκB in generation of alkali burn-induced inflammatory environment, macrophage invasion, and expression of cytokines are increased in alkali burned corneas, and are decreased upon inhibition of NFκB (Saika et al., 2005). Elevated expression of pro-inflammatory cytokines in TNF-α-activated HUVEC cells and alkali burned corneas, and their decreased production in the presence of SLURP1 (Fig. 4) is consistent with cytoplasmic retention of NFκB by SLURP1 (Fig. 7). Previously, we have reported that Slurp1 modulates corneal homeostasis by serving as a soluble scavenger of uPA (Swamynathan and Swamynathan, 2014). Understanding the effect of SLURP1 on *(i)* the stability of IκB which binds NF-κB and inhibits its nuclear localization, *(ii)* upstream signaling pathways that feed into NFκB, *(iii)* the expression of other pro-angiogenic cytokines, and *(iv)* additional factors that interact with SLURP1 will be essential to completely understand the molecular mechanism underlying anti-angiogenic function of SLURP1.

Although CNV occurs in the corneal stroma, many corneal epithelium-expressed factors play important roles in regulating it (Bock et al., 2013; Kinoshita et al., 2001). High level of expression of VEGF-R3 in the corneal epithelium suppresses inflammatory corneal angiogenesis by serving as a sink for VEGF which would otherwise stimulate inflammatory CNV via macrophage recruitment (Cursiefen et al., 2004b, 2006, 2005; Jin et al., 2011). Similarly, corneal epithelial expression of PD-L1 helps block angiogenesis (Jin et al., 2011). Our results add SLURP1 to the list of anti-angiogenic factors in the corneal epithelium, and suggest that SLURP1-based therapy may prove useful in controlling inflammatory CNV. In view of their redundant nature, it will be beneficial to evaluate combinatorial therapy targeting multiple pro- and anti-angiogenic factors such as PD-L1, thrombospondin-1, α5-integrin, and VEGF-A, to manage pathological CNV (Bock et al., 2007; Cursiefen et al., 2011; Dietrich et al., 2007). As the corneal transplants onto vascularized graft beds are rejected at a high frequency (Bachmann et al., 2010), identification of SLURP1 as an anti-angiogenic factor provides a new potential target for decreasing graft rejection. Considering that anti-VEGF therapy increases the corneal graft survival rate (Cursiefen et al., 2004a; Yatoh et al., 1998), and that SLURP1 has potent anti-angiogenic properties, we anticipate that maintaining optimal levels of SLURP1 (either by topical applications or through

stimulating endogenous expression) in the host and the graft corneas is likely to improve graft survival.

5. Conclusions

The results presented in this report *(i)* demonstrate that SLURP1 suppresses HUVEC tube formation by blocking the nuclear translocation of NFκB, *(ii)* suggest a potential role for SLURP1 in promoting corneal angiogenic privilege, and *(iii)* highlight yet another means by which the corneal epithelium contributes to the overall health of the cornea.

Acknowledgments

Funding

This study was supported by NIH Grant R01EY022898 (SKS), NEI Core Grant P30 EY08098, and by unrestricted grants from Research to Prevent Blindness and the Eye and Ear Foundation of Pittsburgh.

The authors thank Kate Davoli (Histology Core Facility) for help with histology, Kira Lathrop (Imaging Core Facility) for help with imaging, and Dr. Anil Tiwari for helpful comments on the manuscript.

Abbreviations used

VEGF	Vascular Endothelial Growth Factor
VEGF-R1	VEGF Receptor-1
SLURP1	Secreted Ly6/urokinase-type plasminogen activator receptor related protein-1
CNV	Corneal Neovascularization
HUVEC	Human Umbilical cord Vascular Endothelial Cell
HCLE	Human Corneal Limbal Epithelial cell
TNF-α	Tumor Necrosis Factor-alpha
TSP	Thrombospondin
PD-L1	Programmed Death Ligand-1
PEDF	Pigment Epithelium Derived Factor
NFκB	Nuclear Factor kappa-B
EBM2	Endodermal Basal Medium-2
EGM2	Endodermal Growth Medium-2
DAPI	4′,6-Diamidino-2-Phenyl-Indole
PVDF	PolyVinyledene DiFluride

References

Adermann K, Wattler F, Wattler S, Heine G, Meyer M, Forssmann WG, Nehls M. Structural and phylogenetic characterization of human SLURP-1, the first secreted mammalian member of the Ly-6/uPAR protein superfamily. Protein Sci Publ Protein Soc. 1999; 8:810–819.

Adeyo O, Allan BB, Barnes RH 2nd, Goulbourne CN, Tatar A, Tu Y, Young LC, Weinstein MM, Tontonoz P, Fong LG, Beigneux AP, Young SG. Palmoplantar keratoderma along with neuromuscular and metabolic phenotypes in Slurp1-deficient mice. J Invest Dermatol. 2014; 134:1589–1598. [PubMed: 24499735]

Ambati BK, Nozaki M, Singh N, Takeda A, Jani PD, Suthar T, Albuquerque RJ, Richter E, Sakurai E, Newcomb MT, Kleinman ME, Caldwell RB, Lin Q, Ogura Y, Orecchia A, Samuelson DA, Agnew DW, St Leger J, Green WR, Mahasreshti PJ, Curiel DT, Kwan D, Marsh H, Ikeda S, Leiper LJ, Collinson JM, Bogdanovich S, Khurana TS, Shibuya M, Baldwin ME, Ferrara N, Gerber HP, De Falco S, Witta J, Baffi JZ, Raisler BJ, Ambati J. Corneal avascularity is due to soluble VEGF receptor-1. Nature. 2006; 443:993–997. [PubMed: 17051153]

Azar DT. Corneal angiogenic privilege: angiogenic and antiangiogenic factors in corneal avascularity, vasculogenesis, and wound healing (an American Ophthalmological Society thesis). Trans Am Ophthalmol Soc. 2006; 104:264–302. [PubMed: 17471348]

Bachmann B, Taylor RS, Cursiefen C. Corneal neovascularization as a risk factor for graft failure and rejection after keratoplasty: an evidence-based meta-analysis. Ophthalmology. 2010; 117:1300–1305. e1307. [PubMed: 20605214]

Barabino S, Chen Y, Chauhan S, Dana R. Ocular surface immunity: homeostatic mechanisms and their disruption in dry eye disease. Prog Retin Eye Res. 2012; 31:271–285. [PubMed: 22426080]

Blasi F, Carmeliet P. uPAR: a versatile signalling orchestrator. Nat Rev Mol Cell Biol. 2002; 3:932–943. [PubMed: 12461559]

Bock F, Maruyama K, Regenfuss B, Hos D, Steven P, Heindl LM, Cursiefen C. Novel anti(lymph)angiogenic treatment strategies for corneal and ocular surface diseases. Prog Retin Eye Res. 2013; 34:89–124. [PubMed: 23348581]

Bock F, Onderka J, Dietrich T, Bachmann B, Kruse FE, Paschke M, Zahn G, Cursiefen C. Bevacizumab as a potent inhibitor of inflammatory corneal angiogenesis and lymphangiogenesis. Invest Ophthalmol Vis Sci. 2007; 48:2545–2552. [PubMed: 17525183]

Chauhan SK, Jin Y, Goyal S, Lee HS, Fuchsluger TA, Lee HK, Dana R. A novel pro-lymphangiogenic function for Th17/IL-17. Blood. 2011; 118:4630–4634. [PubMed: 21908425]

Chimienti F, Hogg RC, Plantard L, Lehmann C, Brakch N, Fischer J, Huber M, Bertrand D, Hohl D. Identification of SLURP-1 as an epidermal neuromodulator explains the clinical phenotype of Mal de Meleda. Hum Mol Genet. 2003; 12:3017–3024. [PubMed: 14506129]

Clements JL, Dana R. Inflammatory corneal neovascularization: etiopathogenesis. Semin Ophthalmol. 2011; 26:235–245. [PubMed: 21958169]

Cursiefen C, Cao J, Chen L, Liu Y, Maruyama K, Jackson D, Kruse FE, Wiegand SJ, Dana MR, Streilein JW. Inhibition of hemangiogenesis and lymphangiogenesis after normal-risk corneal transplantation by neutralizing VEGF promotes graft survival. Invest Ophthalmol Vis Sci. 2004a; 45:2666–2673. [PubMed: 15277490]

Cursiefen C, Chen L, Borges LP, Jackson D, Cao J, Radziejewski C, D'Amore PA, Dana MR, Wiegand SJ, Streilein JW. VEGF-A stimulates lymphangiogenesis and hemangiogenesis in inflammatory neovascularization via macrophage recruitment. J Clin Invest. 2004b; 113:1040–1050. [PubMed: 15057311]

Cursiefen C, Chen L, Saint-Geniez M, Hamrah P, Jin Y, Rashid S, Pytowski B, Persaud K, Wu Y, Streilein JW, Dana R. Nonvascular VEGF receptor 3 expression by corneal epithelium maintains avascularity and vision. Proc Natl Acad Sci U S A. 2006; 103:11405–11410. [PubMed: 16849433]

Cursiefen C, Ikeda S, Nishina PM, Smith RS, Ikeda A, Jackson D, Mo JS, Chen L, Dana MR, Pytowski B, Kruse FE, Streilein JW. Spontaneous corneal hem- and lymphangiogenesis in mice with destrin-mutation depend on VEGFR3 signaling. Am J Pathol. 2005; 166:1367–1377. [PubMed: 15855638]

Cursiefen C, Maruyama K, Bock F, Saban D, Sadrai Z, Lawler J, Dana R, Masli S. Thrombospondin 1 inhibits inflammatory lymphangiogenesis by CD36 ligation on monocytes. J Exp Med. 2011; 208:1083–1092. [PubMed: 21536744]

Defilippi P, Silengo L, Tarone G. Alpha 6. beta 1 integrin (laminin receptor) is down-regulated by tumor necrosis factor alpha and interleukin-1 beta in human endothelial cells. J Biol Chem. 1992; 267:18303–18307. [PubMed: 1388151]

Defilippi P, Truffa G, Stefanuto G, Altruda F, Silengo L, Tarone G. Tumor necrosis factor alpha and interferon gamma modulate the expression of the vitronectin receptor (integrin beta 3) in human endothelial cells. J Biol Chem. 1991; 266:7638–7645. [PubMed: 1708389]

Dietrich T, Onderka J, Bock F, Kruse FE, Vossmeyer D, Stragies R, Zahn G, Cursiefen C. Inhibition of inflammatory lymphangiogenesis by integrin alpha5 blockade. Am J Pathol. 2007; 171:361–372. [PubMed: 17591980]

Eckl KM, Stevens HP, Lestringant GG, Westenberger-Treumann M, Traupe H, Hinz B, Frossard PM, Stadler R, Leigh IM, Nurnberg P, Reis A, Hennies HC. Mal de Meleda (MDM) caused by mutations in the gene for SLURP-1 in patients from Germany, Turkey, Palestine, and the United Arab Emirates. Hum Genet. 2003; 112:50–56. [PubMed: 12483299]

El Annan J, Goyal S, Zhang Q, Freeman GJ, Sharpe AH, Dana R. Regulation of T-cell chemotaxis by programmed death-ligand 1 (PD-L1) in dry eyeassociated corneal inflammation. Invest Ophthalmol Vis Sci. 2010; 51:3418–3423. [PubMed: 20019373]

Favre B, Plantard L, Aeschbach L, Brakch N, Christen-Zaech S, de Viragh PA, Sergeant A, Huber M, Hohl D. SLURP1 is a late marker of epidermal differentiation and is absent in Mal de Meleda. J Invest Dermatol. 2007; 127:301–308. [PubMed: 17008884]

Fibbi G, Caldini R, Chevanne M, Pucci M, Schiavone N, Morbidelli L, Parenti A, Granger HJ, Del Rosso M, Ziche M. Urokinase-dependent angiogenesis in vitro and diacylglycerol production are blocked by antisense oligonucleotides against the urokinase receptor. Lab Investig J Tech Methods Pathol. 1998; 78:1109–1119.

Fischer J, Bouadjar B, Heilig R, Huber M, Lefevre C, Jobard F, Macari F, Bakija-Konsuo A, Ait-Belkacem F, Weissenbach J, Lathrop M, Hohl D, Prud'homme JF. Mutations in the gene encoding SLURP-1 in Mal de Meleda. Hum Mol Genet. 2001; 10:875–880. [PubMed: 11285253]

Fujii T, Horiguchi K, Sunaga H, Moriwaki Y, Misawa H, Kasahara T, Tsuji S, Kawashima K. SLURP-1, an endogenous alpha7 nicotinic acetylcholine receptor allosteric ligand, is expressed in CD205(+) dendritic cells in human tonsils and potentiates lymphocytic cholinergic activity. J Neuroimmunol. 2014; 267:43–49. [PubMed: 24365495]

Horiguchi K, Horiguchi S, Yamashita N, Irie K, Masuda J, Takano-Ohmuro H, Himi T, Miyazawa M, Moriwaki Y, Okuda T, Misawa H, Ozaki H, Kawashima K. Expression of SLURP-1, an endogenous alpha7 nicotinic acetylcholine receptor allosteric ligand, in murine bronchial epithelial cells. J Neurosci Res. 2009; 87:2740–2747. [PubMed: 19396877]

Hu G, Yildirim M, Baysal V, Yerebakan O, Yilmaz E, Inaloz HS, Martinez-Mir A, Christiano AM, Celebi JT. A recurrent mutation in the ARS (component B) gene encoding SLURP-1 in Turkish families with mal de Meleda: evidence of a founder effect. J Invest Dermatol. 2003; 120:967–969. [PubMed: 12787122]

Jia C, Zhu W, Ren S, Xi H, Li S, Wang Y. Comparison of genome-wide gene expression in suture- and alkali burn-induced murine corneal neo-vascularization. Mol Vis. 2011; 17:2386–2399. [PubMed: 21921991]

Jin Y, Chauhan SK, El Annan J, Sage PT, Sharpe AH, Dana R. A novel function for programmed death ligand-1 regulation of angiogenesis. Am J Pathol. 2011; 178:1922–1929. [PubMed: 21435468]

Keir ME, Butte MJ, Freeman GJ, Sharpe AH. PD-1 and its ligands in tolerance and immunity. Annu Rev Immunol. 2008; 26:677–704. [PubMed: 18173375]

Kinoshita S, Adachi W, Sotozono C, Nishida K, Yokoi N, Quantock AJ, Okubo K. Characteristics of the human ocular surface epithelium. Prog Retin Eye Res. 2001; 20:639–673. [PubMed: 11470454]

Kubota M, Shimmura S, Kubota S, Miyashita H, Kato N, Noda K, Ozawa Y, Usui T, Ishida S, Umezawa K, Kurihara T, Tsubota K. Hydrogen and N-acetyl-L-cysteine rescue oxidative stress-

induced angiogenesis in a mouse corneal alkali-burn model. Invest Ophthalmol Vis Sci. 2011; 52:427–433. [PubMed: 20847117]

Lee P, Wang CC, Adamis AP. Ocular neovascularization: an epidemiologic review. Surv Ophthalmol. 1998; 43:245–269. [PubMed: 9862312]

Lim P, Fuchsluger TA, Jurkunas UV. Limbal stem cell deficiency and corneal neovascularization. Semin Ophthalmol. 2009; 24:139–148. [PubMed: 19437349]

Loughner CL, Bruford EA, McAndrews MS, Delp EE, Swamynathan S, Swamynathan SK. Organization, evolution and functions of the human and mouse Ly6/uPAR family genes. Hum genomics. 2016; 10:10. [PubMed: 27098205]

Ma DH, Chen JK, Zhang F, Lin KY, Yao JY, Yu JS. Regulation of corneal angiogenesis in limbal stem cell deficiency. Prog Retin Eye Res. 2006; 25:563–590. [PubMed: 17079182]

Maruyama K, Ii M, Cursiefen C, Jackson DG, Keino H, Tomita M, Van Rooijen N, Takenaka H, D'Amore PA, Stein-Streilein J, Losordo DW, Streilein JW. Inflammation-induced lymphangiogenesis in the cornea arises from CD11b-positive macrophages. J Clin Invest. 2005; 115:2363–2372. [PubMed: 16138190]

Maruyama K, Nakazawa T, Cursiefen C, Maruyama Y, Van Rooijen N, D'Amore PA, Kinoshita S. The maintenance of lymphatic vessels in the cornea is dependent on the presence of macrophages. Invest Ophthalmol Vis Sci. 2012; 53:3145–3153. [PubMed: 22511631]

Mastrangeli R, Donini S, Kelton CA, He C, Bressan A, Milazzo F, Ciolli V, Borrelli F, Martelli F, Biffoni M, Serlupi-Crescenzi O, Serani S, Micangeli E, El Tayar N, Vaccaro R, Renda T, Lisciani R, Rossi M, Papoian R. ARS Component B: structural characterization, tissue expression and regulation of the gene and protein (SLURP-1) associated with Mal de Meleda. Eur J Dermatol. 2003; 13:560–570. [PubMed: 14721776]

Matsumoto H, Shibasaki K, Uchigashima M, Koizumi A, Kurachi M, Moriwaki Y, Misawa H, Kawashima K, Watanabe M, Kishi S, Ishizaki Y. Localization of acetylcholine-related molecules in the retina: implication of the communication from photoreceptor to retinal pigment epithelium. PLoS One. 2012; 7:e42841. [PubMed: 22880119]

Montuori N, Ragno P. Role of uPA/uPAR in the modulation of angiogenesis. Chem Immunol Allergy. 2014; 99:105–122. [PubMed: 24217605]

Moriwaki Y, Watanabe Y, Shinagawa T, Kai M, Miyazawa M, Okuda T, Kawashima K, Yabashi A, Waguri S, Misawa H. Primary sensory neuronal expression of SLURP-1, an endogenous nicotinic acetylcholine receptor ligand. Neurosci Res. 2009; 64:403–412. [PubMed: 19409425]

Moriwaki Y, Yoshikawa K, Fukuda H, Fujii YX, Misawa H, Kawashima K. Immune system expression of SLURP-1 and SLURP-2, two endogenous nicotinic acetylcholine receptor ligands. Life Sci. 2007; 80:2365–2368. [PubMed: 17286989]

Morris JE, Zobell S, Yin XT, Zakeri H, Summers BC, Leib DA, Stuart PM. Mice with mutations in Fas and Fas ligand demonstrate increased herpetic stromal keratitis following corneal infection with HSV-1. J Immunol. 2012; 188:793–799. [PubMed: 22156346]

Norman B, Davis J, Piatigorsky J. Postnatal gene expression in the normal mouse cornea by SAGE. Invest Ophthalmol Vis Sci. 2004; 45:429–440. [PubMed: 14744882]

Parikh T, Eisner N, Venugopalan P, Yang Q, Lam BL, Bhattacharya SK. Proteomic analyses of corneal tissue subjected to alkali exposure. Invest Ophthalmol Vis Sci. 2011; 52:1819–1831. [PubMed: 20861482]

Reynolds AB, Kanner SB, Bouton AH, Schaller MD, Weed SA, Flynn DC, Parsons JT. SRCing for the substrates of Src. Oncogene. 2014; 33:4537–4547. [PubMed: 24121272]

Rotundo RF, Curtis TM, Shah MD, Gao B, Mastrangelo A, LaFlamme SE, Saba TM. TNF-alpha disruption of lung endothelial integrity: reduced integrin mediated adhesion to fibronectin. American journal of physiology Lung Cell Mol Physiol. 2002; 282:L316–L329.

Saika S, Miyamoto T, Yamanaka O, Kato T, Ohnishi Y, Flanders KC, Ikeda K, Nakajima Y, Kao WW, Sato M, Muragaki Y, Ooshima A. Therapeutic effect of topical administration of SN50, an inhibitor of nuclear factor-kappaB, in treatment of corneal alkali burns in mice. Am J Pathol. 2005; 166:1393–1403. [PubMed: 15855640]

Smith HW, Marshall CJ. Regulation of cell signalling by uPAR. Nat Rev Mol Cell Biol. 2010; 11:23–36. [PubMed: 20027185]

Sotozono C, He J, Matsumoto Y, Kita M, Imanishi J, Kinoshita S. Cytokine expression in the alkali-burned cornea. Curr Eye Res. 1997; 16:670–676. [PubMed: 9222084]

Stuart PM, Pan F, Plambeck S, Ferguson TA. FasL-Fas interactions regulate neovascularization in the cornea. Invest Ophthalmol Vis Sci. 2003; 44:93–98. [PubMed: 12506060]

Swamynathan S, Buela KA, Kinchington P, Lathrop KL, Misawa H, Hendricks RL, Swamynathan SK. Klf4 regulates the expression of Slurp1, which functions as an immunomodulatory peptide in the mouse cornea. Invest Ophthalmol Vis Sci. 2012; 53:8433–8446. [PubMed: 23139280]

Swamynathan S, Delp EE, Harvey SA, Loughner CL, Raju L, Swamynathan SK. Corneal expression of SLURP-1 by age, sex, genetic strain, and ocular surface health. Invest Ophthalmol Vis Sci. 2015; 56:7888–7896. [PubMed: 26670825]

Swamynathan S, Swamynathan SK. SLURP-1 modulates corneal homeostasis by serving as a soluble scavenger of urokinase-type plasminogen activator. Invest Ophthalmol Vis Sci. 2014; 55:6251–6261. [PubMed: 25168896]

Tandon A, Tovey JC, Sharma A, Gupta R, Mohan RR. Role of transforming growth factor Beta in corneal function, biology and pathology. Curr Mol Med. 2010; 10:565–578. [PubMed: 20642439]

Ward KM, Yerebakan O, Yilmaz E, Celebi JT. Identification of recurrent mutations in the ARS (component B) gene encoding SLURP-1 in two families with mal de Meleda. J Invest Dermatol. 2003; 120:96–98. [PubMed: 12535203]

Yatoh S, Kawakami Y, Imai M, Kozawa T, Segawa T, Suzuki H, Yamashita K, Okuda Y. Effect of a topically applied neutralizing antibody against vascular endothelial growth factor on corneal allograft rejection of rat. Transplantation. 1998; 66:1519–1524. [PubMed: 9869094]

Yoshizuka M, Katsume Y, Fujimoto S, Ogoh Y. Dynamic changes of the corneal epithelium and stroma after alkali burning. Kurume Med J. 1981; 28:23–27. [PubMed: 6172633]

Zhang MC, Wang Y, Yang Y. The expression of nuclear factor kappa B in inflammation-induced rat corneal neovascularization. Ocul Immunol Inflamm. 2006; 14:359–365. [PubMed: 17162607]

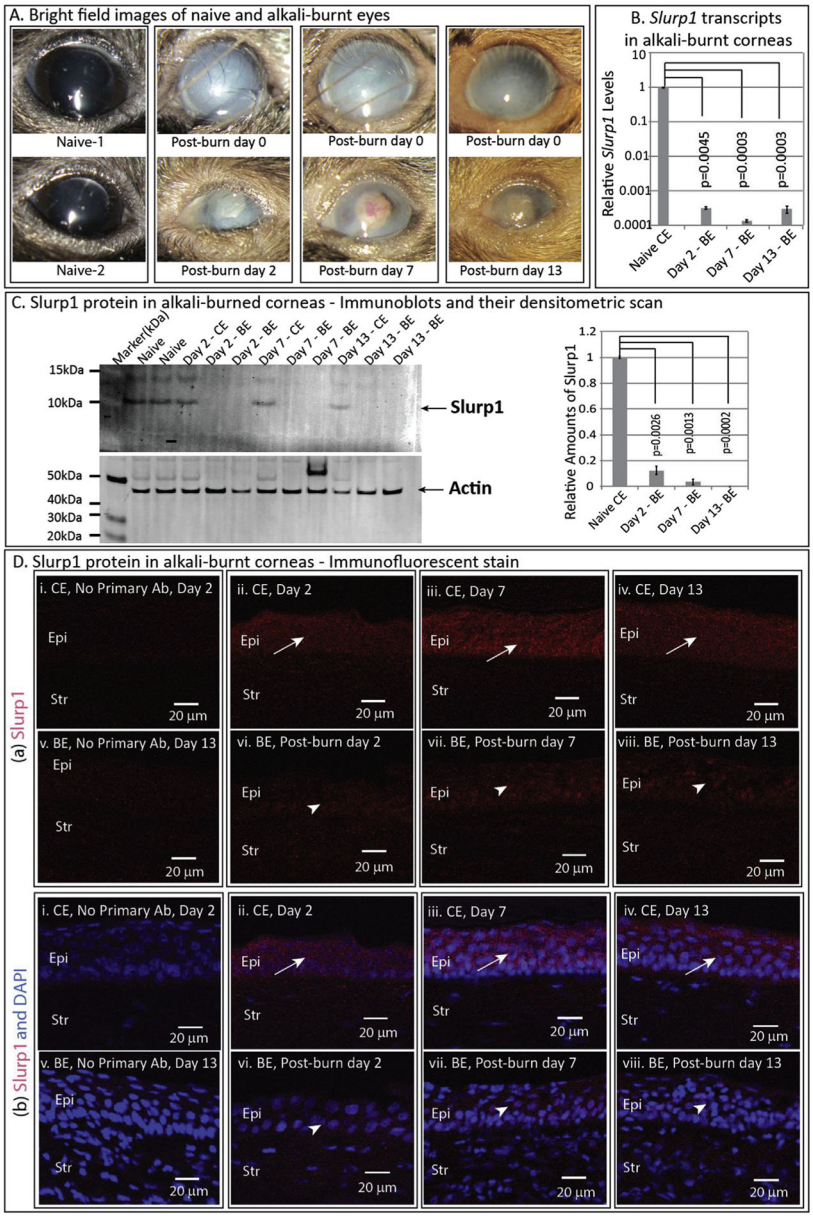

Fig. 1. Effect of alkali-burn on Slurp1expression in mouse corneas

(A) Bright field images of naïve and alkali-burned eyes at post-burn days 0, 2, 7 and 13 showing their external appearance. Note that CNV is apparent by post-burn day 7, and persists at day 13. (B) *Slurp1* transcript levels in corneas from alkali-burned eyes (BE) relative to that in corneas from naïve contralateral eyes (CE) on post-burn days 2, 7 and 13, quantified by QPCR using pyruvate carboxylase (PCX) as endogenous control and plotted on log scale. (C) Slurp1 protein on post-burn days 2, 7 and 13, detected by immunoblots with anti-Slurp1 antibody (white arrow). The blot was re-probed with anti-actin antibody for loading control (black arrow). Slurp1:Actin signal intensity ratios determined by densitometry are shown on the right side, reflecting relative amounts of Slurp1 protein in alkali-burned corneas. (D) Slurp1 protein in mouse corneas on post-burn days 2, 7 and 13,

detected by immunofluorescent stain with anti-Slurp1 antibody (red). Nuclei were counterstained blue by DAPI. Images procured from sections incubated with no primary antibody controls are shown (Di and Dv). Note that corneal epithelial expression of Slurp1 is abundant in the control (Dii-Div; arrows) and sharply decreased in alkali-burned (Dvi–Dviii; arrowheads) corneas. BE, Alkali-burned eye; CE, Contralateral eye. Scale bar, 20 μm. (For interpretation of the references to colour in this figure legend, the reader is referred to the web version of this article.)

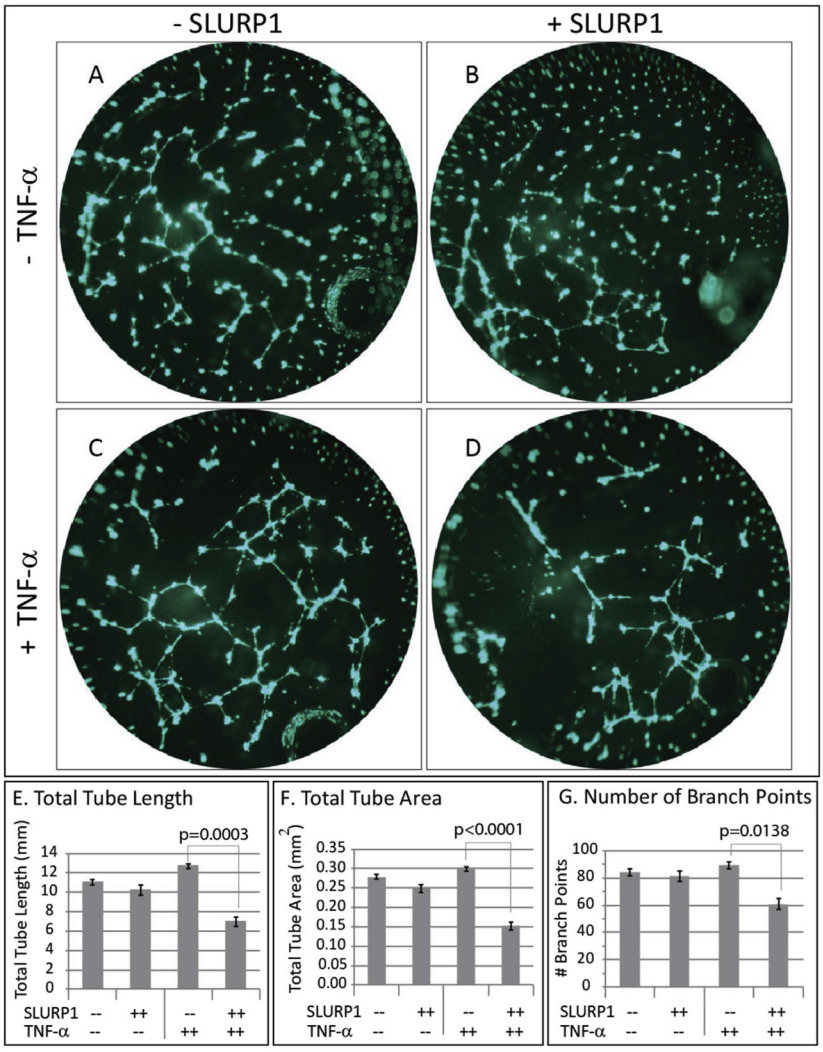

Fig. 2.

Effect of SLURP1 on TNF-α induced tube formation in HUVEC cells. (A–D) HUVEC cells pre-treated with control protein, or SLURP1 and seeded on matrigel in the presence of control protein (A and C) or SLURP1 (B and D) were allowed to form tubes for 18 h in the presence (C and D) or absence (A and B) of TNF-α. Images were taken after treating with calcein-AM. Images are representative of five different experiments. Total tube length (E), total tube area (F), and the number of branch points (G) in captured images were measured using MetaMorph. Data shown are the average of six independent replicates.

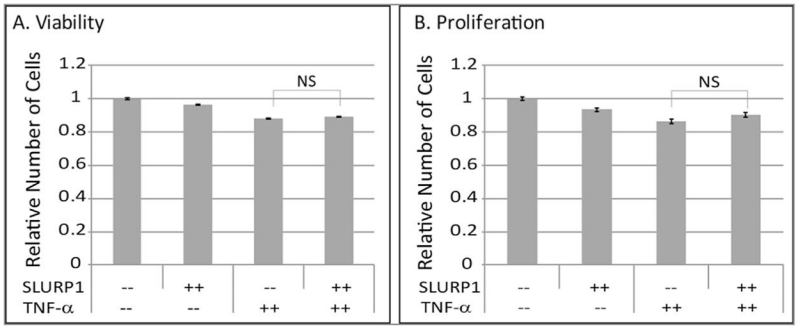

Fig. 3.

SLURP1 does not affect the viability and proliferation of HUVEC cells. (A) Viability and (B) proliferation of HUVEC cells were measured over 24 h period in the presence of control protein and SLURP1 and with and without TNF-α treatment. Data shown are the average of three experiments.

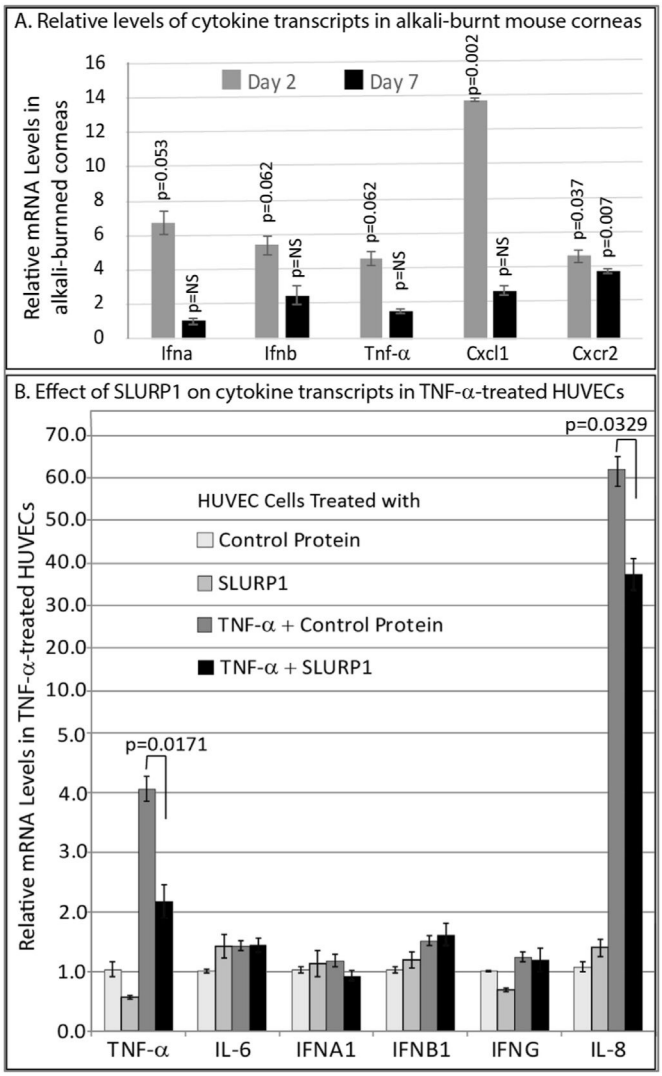

Fig. 4. Relative cytokine levels in alkali burned corneas and the effect of SLURP1 on TNF-α-induced cytokine expression in HUVEC

A. Relative levels of transcripts encoding Ifna, Ifnb, Tnfa, Cxcl1 and Cxcr2 in alkali-burned mouse corneas on post-burn days-2 and -7. RNA was extracted from control contralateral and alkali-burned mouse corneas on post-burn days-2 and -7, and the transcript levels tested by QPCR. B. Compound panel chart showing the effect of SLURP1 on expression of different cytokine transcripts in HUVEC cells. RNA was extracted from HUVEC cells pretreated with SLURP1 or control protein and exposed to TNF-α for 4 h and transcript levels measured by QPCR. Y-axis is presented as a compound panel, with the scale shifting to multiples of 10 after 5, to accommodate the large increase in IL-8 expression in HUVEC cells following TNF-α treatment. Results shown are the average of three independent experiments.

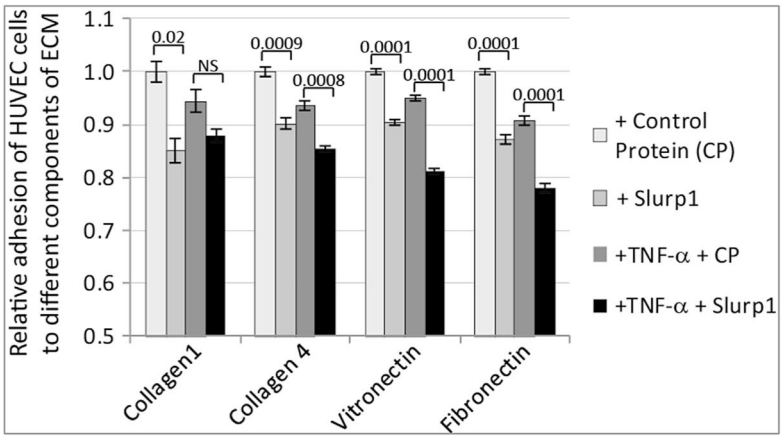

Fig. 5.

Effect of SLURP1 on adhesion of HUVEC cells to different components of extra cellular matrix. HUVEC cells were pre-treated with control protein or SLURP1 and TNF-α, and subjected to adhesion assay. Results shown are representative of three independent experiments.

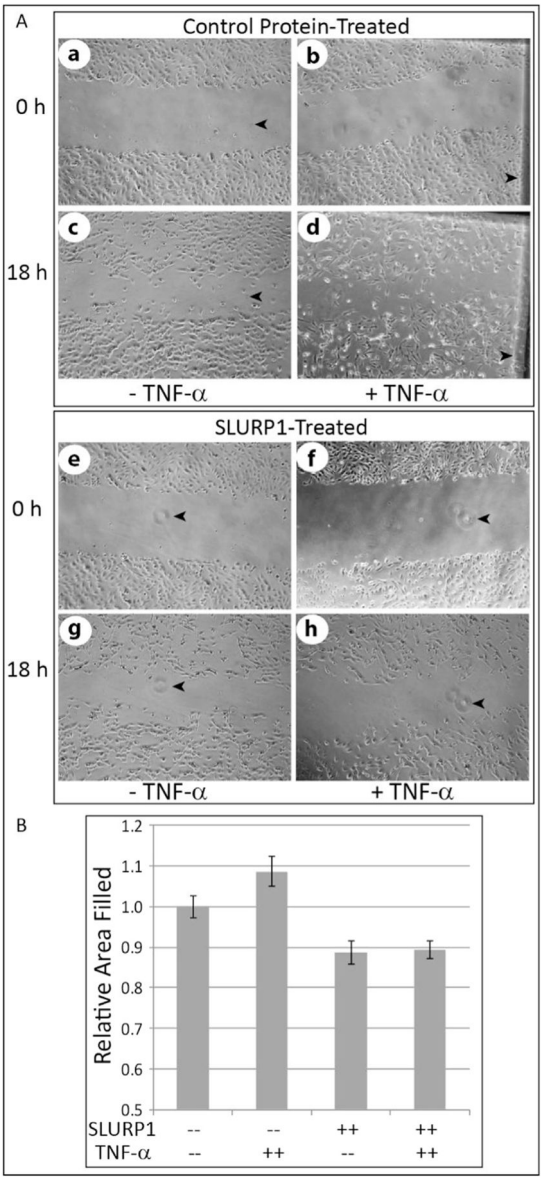

Fig. 6.

Effect of SLURP1 on HUVEC cell migration. Gaps were generated in confluent HUVEC cells treated with control protein or SLURP1 and stimulated with TNF-α. Images captured from the same spots (detected using reference markings just outside of the imaged areas; also discerned using background marks indicated by arrowheads) at 0 h and after 18 h of gap-filling were used to quantify the relative area filled in. Representative images are shown on the top (A), and the mean results from four replicates are shown at the bottom (B).

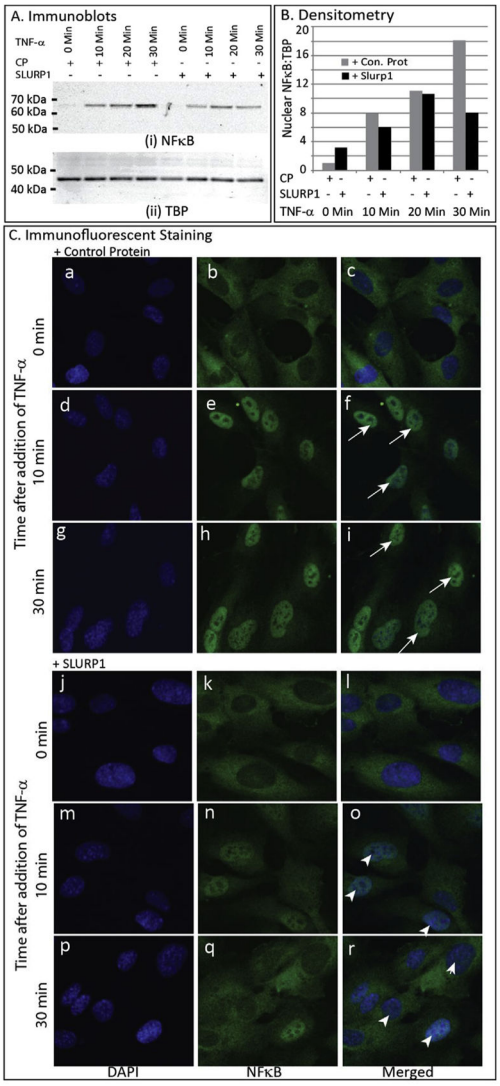

Fig. 7.

Effect of SLURP1 on TNF-α-induced nuclear localization of NFκB in HUVEC cells. (A) Immunoblots with HUVEC nuclear extracts (blots probed with anti-NFκB and anti-TBP antibody). HUVEC cells were pre-treated with control protein or SLURP1 for 30 min, exposed to TNF-α, nuclear extract prepared at 0, 10, 20 and 30 min after TNF-α treatment, separated by SDS-PAGE, and NFκB and TBP detected by immunoblots as indicated. (B) Relative quantities of nuclear NFκB estimated by densitometric scans. NFκB and TBP band intensities were quantified by densitometric scans and NFκB:TBP ratios plotted. (C) Immunofluorescent Staining for NFκB. HUVEC cells were pre-treated with control protein (a–i) or SLURP1 (j–r) for 30 min, exposed to TNF-α, fixed at 0,10, and 30 min after TNF-α treatment, and the sub-cellular localization of NFκB detected by immunofluorescent staining (green). Nuclei are stained blue with DAPI (blue). TNF-α induced nuclear localization of NFκB in control protein treated HUVEC cells within 10 min (f and i; arrows) but not in SLURP1-treated cells, where it remained within the cytoplasm even after 30 min

of treatment (o and r; arrowheads). (For interpretation of the references to colour in this figure legend, the reader is referred to the web version of this article.)

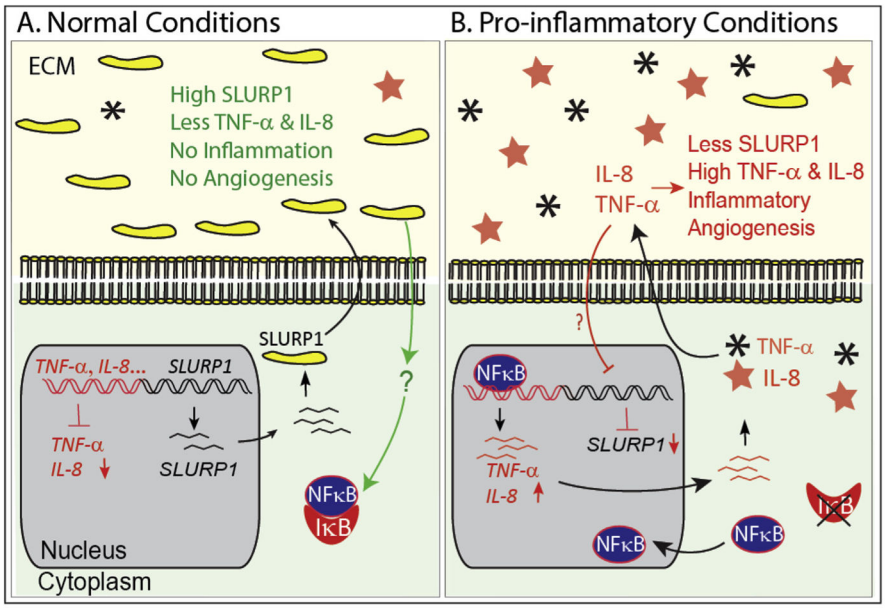

Fig. 8.

Schematic representation of the involvement of SLURP1 in regulating inflammatory angiogenesis. (A) In normal conditions, abundance of SLURP1 results in low level of pro-inflammatory cytokines such as TNF-α and IL-8, which in turn allows cytoplasmic retention of NFκB by binding of IκB. Signaling events that connect SLURP1 and NFκB remain to be elucidated, and are indicated by a question mark. (B) SLURP1 expression is downregulated in pro-inflammatory conditions allowing nuclear localization of NFκB that further stimulates the expression of pro-angiogenic factors and inflammatory angiogenesis. ECM, extracellular matrix.